

Research Article | Diamond Open Access

July 2024 | CC-BY 4.0 | Issue 01: Article 01

DOI: <https://doi.org/10.63024/m9wk-3420>

Projecting future tropical cyclone frequencies by combining uncertain empirical estimates of baseline frequencies with climate model estimates of change

Stephen Jewson¹

¹Lambda Climate Research Ltd., London, UK

Corresponding author email: stephen.jewson@gmail.com

Abstract

Various studies have given projections for how frequencies of tropical cyclones (TCs) might change under climate change. In this study, we combine a set of such projections with uncertain estimates of frequencies of tropical cyclones in a baseline climate to produce probabilistic projections of tropical cyclone frequencies for the next 50 years. The novel aspect of our projections is the inclusion of baseline uncertainty. We consider frequencies of Saffir-Simpson Hurricane Wind Scale category 0-5 and category 4-5 storms for the six major tropical cyclone basins. We find that in several cases the means and medians of the frequency of category 0-5 storms are projected to decrease, but that increasing uncertainty nevertheless leads to increases in the likelihood of high rates of TC activity in the future.

We then show how the variance of the distributions of uncertainty can be decomposed into terms due to baseline uncertainty and climate change uncertainty. We use this decomposition to determine the year in which climate change uncertainty overtakes baseline uncertainty. Over the next 20 years we find that in some basins baseline uncertainty dominates and in other basins climate change uncertainty dominates. We are able to relate these variations between basins to the coefficients of variation of the baseline and climate change inputs. Finally, we quantify how climate change affects estimates of near-term TC frequency, including the extent to which it increases the uncertainty. These results help us understand two of the major sources of uncertainty in estimates of tropical cyclone behaviour now and in the future, and the role climate change is playing in changing that behaviour. They also demonstrate how estimates of TC change can be combined with observations to create projections of future TC climate.

Key Points

1. Projections of future climate often consist of an estimate of a baseline climate plus an estimate of change from the baseline climate. Both are uncertain.
2. We create projections of future hurricane frequencies by combining estimates of a baseline climate with estimates of climate change.
3. Initially, baseline uncertainty dominates the total uncertainty. Later, climate change uncertainty dominates.

1. Introduction

There is great interest in understanding the risks caused by tropical cyclones (TCs), both now and in the future. Following the pioneering work of Don Friedman (1972), there have been many studies that have investigated how to develop models, or components of models, for understanding TC risks. These include Friedman (1975), Clark (1986), Vickery et al. (2000), Jagger and Elsner (2006), Emanuel et al. (2006), Hall and Jewson (2007), Grieser and Jewson (2012), Lee et al. (2018), Bloemendaal et al. (2020) and Arthur (2021). In addition, TC risk models have been developed in the insurance industry, and aspects of those models are described in the materials published by the Florida Commission on Hurricane Loss Projection Methodology (FSBoA, 2022).

Many researchers have also tried to understand how TCs may be changing because of climate change. Recent studies include those by Sun et al. (2017), Liu et al. (2019), Bhatia et al. (2019), Stansfield et al. (2020), Emanuel (2020), Murakami et al. (2020), Zhang et al. (2020), Hassanzadeh et al. (2020), Yamaguchi et al. (2020) and Garner et al. (2021). Reviews of the possible impacts of climate change on TC behaviour have been given by Walsh et al. (2015) and Knutson et al. (2019; 2020). There have also been some attempts to understand how TC risk may be changing because of climate change, where risk is expressed in terms of either windspeed (Bloemendaal, et al., 2022) or in terms of financial damage (Jewson, 2023; Meiler, et al., 2023).

One major focus of TC research has been TC frequency (Sobel, et al., 2021). TC frequency is of particular interest to risk modellers in insurance, since it is an exposed variable in many insurance risk models. Users of TC risk models often adjust the characteristics of the model by adjusting the frequencies of different types of events (Jewson, 2022). There have been many efforts to understand what we can say about baseline TC frequency from

historical data, such as Elsner and Jagger (2006), Jewson et al. (2007), Coughlin et al. (2009), Villarini et al. (2012), Tolwinski-Ward (2015), Ting et al. (2019) and Kaczmarek et al. (2022).

In this study, we seek to gain further understanding of future TC frequencies and how they can be estimated. A meta-study based on previous results relating to possible changes in TC frequency was described by Knutson et al. (2020) (henceforth K2020). The studies considered by K2020 all gave estimates of possible *changes* in TC frequencies due to climate change. To use the results from these studies to derive projections of *actual* future TC frequencies requires them to be combined with estimates of a baseline climate derived from historical data. Projections created in this way, that project values of actual future TC frequencies, may be more useful for risk assessment than projections that just give changes, and we therefore investigate how to construct such projections. We also focus on understanding how the uncertainties in the estimates of the baseline climate combine with the uncertainties in the estimates of change to generate estimates of future uncertainty. Combining baseline and change uncertainties is a step towards including all the readily quantifiable uncertainties in projections of future TC activity, which should lead to better decision making with respect to future TC risk.

We consider the impact of climate change on TC frequency for Saffir-Simpson Hurricane Wind Scale category 0-5 (cat05) and category 4-5 (cat45) storms, separately for the six major TC basins, giving 12 cases. We combine empirical estimates of baseline TC frequencies, based on statistical analysis of data from IBTrACS (International Best Track Archive for Climate Stewardship, Knapp, et al., 2010), with projections of possible changes in TC frequency, derived from the K2020 meta-study results. This allows us to create distributions of possible future TC activity that incorporate both baseline uncertainty and climate change uncertainty. To further

understand these projections, we then decompose the variance of the uncertainty in our estimates into three terms, which are related to baseline uncertainty, climate change uncertainty and the interaction of the two. This allows us to determine the point at which climate change uncertainty overtakes baseline uncertainty as the most important driver of the combined uncertainty. It also allows us to evaluate the contribution of the interaction term, and how climate change affects estimates of near-term climate.

In Section 2 we discuss the historical data we use, and the estimation of the baseline TC frequency distributions. In Section 3 we discuss the climate change information we use, and how we post-process it for use in this study. In Section 4 we combine the baseline frequency distributions with the distributions of change to create projected frequency distributions. In Section 5 we decompose the variance of the projections and consider the implications of our results for near future climate. In Section 6 we discuss the uncertainties around our results and in Section 7 we summarise and conclude.

2. Historical Data and Baseline Frequency Uncertainty

2.1. IBTrACS Data

Our estimates of baseline climate will be derived from the IBTrACS data set, which provides information for global TCs from 1840 to the present. We extract the maximum intensity of each storm during this period for our analysis. In some cases, IBTrACS contains multiple estimates of TC characteristics for each storm, as produced by different agencies around the world. We use the intensity estimates referred to as the 'US representative agency' data. This data is from the National Hurricane Center for the North Atlantic and Eastern North Pacific, the Central Pacific Hurricane Center for the central North Pacific, and the Joint Typhoon Warning Center for the other TC basins. If we were to use the alternative

estimates from within IBTrACS then both the mean numbers of cat05 and cat45 storms, and the uncertainty around the mean, would likely be somewhat different. Our decision to use the US representative agency data is essentially arbitrary, and this is therefore a source of uncertainty with respect to the quantification of the baseline climate. This uncertainty could be explored by repeating our analysis with different datasets, or by weighting and blending the different datasets. That would require detailed exploration of the nature of and reasons for the differences between the different datasets, and is beyond the scope of this study.

We use the IBTrACS definitions of basin boundaries, and data from 1980 to 2021, since 1980 is the approximate start of global monitoring of TCs from geostationary and polar-orbiting satellites. We will ignore the possible impact of changes in measurement technology and reporting practice that may have occurred during the period from 1980 to 2021, since, to our knowledge, the possible impacts of such changes have not been well quantified.

2.2. Baseline Frequency Uncertainty

We derive our estimates of the mean baseline climate, in terms of frequency of cat05 and cat45 storms, as follows. First, we categorise every historical storm from IBTrACS as cat05 and/or cat45. We consider cat05s and cat45s in order to be consistent with the information given in K2020. As is standard, cat05 is defined as storms with reported maximum intensity of 34 knots or higher, and cat45 is defined as storms with reported maximum intensity of 113 knots or higher. The mean numbers of cat05 and cat45 storms per year, and various other statistics that will be useful for our subsequent analyses, are given in Table 1.

Our estimates of the mean climate average over subseasonal, seasonal and interannual variability, which is appropriate, since we are interested in projections of future climate further into the future than any of these types of variability are predictable.

Table 1: Observed tropical cyclone (TC) statistics derived from IBTrACS data for 1980-2021, for the six main TC basins, for category 0-5 and category 4-5 storms. Column 3 gives the observed number of storms, column 4 gives the mean number of storms per year over the 42 year period, column 5 gives the estimated standard deviation of the number of storms per year, column 6 gives the estimated standard error of the mean number of storms per year, column 7 expresses column 6 as a percentage of the mean and column 8 gives the dispersion, defined as the ratio of the variance of the number of storms per year to the mean number of storms per year

BASIN	CATEGORY	NUMBER OF HISTORICAL STORMS, 1980-2021	MEAN # STORMS PER YEAR	SD # STORMS PER YEAR	SE # STORMS PER YEAR	SE AS % OF MEAN	DISPERSION (VARIANCE / MEAN)
NA	cat05	564	13.43	5.56	0.86	6.39	2.3
NA	cat45	72	1.71	1.5	0.23	13.53	1.32
NWP	cat05	1110	26.43	4.58	0.71	2.67	0.79
NWP	cat45	292	6.95	2.92	0.45	6.48	1.23
NEP	cat05	738	17.57	4.63	0.71	4.06	1.22
NEP	cat45	129	3.07	2.46	0.38	12.38	1.98
NI	cat05	215	5.12	1.8	0.28	5.42	0.63
NI	cat45	24	0.57	0.7	0.11	18.99	0.87
SI	cat05	686	16.33	3.35	0.52	3.17	0.69
SI	cat45	119	2.83	2.13	0.33	11.59	1.6
SP	cat05	404	9.62	3.57	0.55	5.73	1.33
SP	cat45	56	1.33	1.24	0.19	14.38	1.16

The sample standard deviation s of the number of storms per year p , given n years of historical storm numbers p_1, p_2, \dots, p_n , with sample mean μ , is given by the usual formula:

$$s = \sqrt{\frac{1}{n-1} \sum_{i=1}^n (p_i - \mu)^2} \quad (1)$$

We neglect the possible impact of climate change during the historical period on this estimated standard deviation, since the impact is likely much

smaller than internal climate variability. We will, however, consider the impact of climate change on the mean during the historical period in our analysis below.

We then consider how to estimate the distribution of uncertainty around the mean number of storms per year μ , since it is this distribution that we will combine with projections of climate change to derive our projections of future climate conditions. This distribution – the distribution of uncertainty of the estimate of the mean – is different from the distribution of the number of storms per year p , and

is much narrower. To distinguish between these two distributions, we will refer to the distribution of the number of storms per year as the *frequency distribution*, and the distribution of uncertainty of the estimate of the mean number of storms per year as the *mean frequency distribution*. The standard deviation of the frequency distribution is given by the equation above. The standard deviation of the mean frequency distribution is the standard deviation of μ , rather than the standard deviation of p . We will discuss how to estimate the standard deviation of μ below.

To illustrate the difference between the frequency distribution and the mean frequency distribution, we now give estimates of both for the North Atlantic. For the frequency distribution, an empirical frequency distribution derived from the IBTrACS data gives frequencies from four storms per year to 30 storms per year, with a mean of 13.4 storms per year. The mean frequency distribution encapsulates the idea that this mean number of storms per year is uncertain: one of the estimates of the uncertainty that we derive below gives it a range from around 11.8 storms per year to around 15.2 storms per year.

We do not attempt to make projections of any aspects of the TC frequency distribution other than the mean, since K2020 only gives projections for changes in the mean. In the future, one might imagine using climate models to extract projections for changes in aspects of the TC frequency distribution other than just the mean, such as changes in variances of TC numbers, or changes in correlations of TC numbers between basins.

2.3. Estimating the Mean Frequency Distribution

We compare two methods for estimating the mean frequency distribution. The first method is based on the commonly used assumption that the TC frequency distribution follows a Poisson distribution. We use Bayesian statistics to derive the mean frequency distribution from that assumption (see Bernardo and Smith (1993), page 437).

The second method makes no assumption about the TC frequency distribution, and uses a method known as the normal approximation to the posterior distribution (see Bernardo and Smith (1993), page 287). In both cases we assume that the storm counts in different historical years are independent. This independence assumption is not likely to be completely true, as it ignores long time-scale variability in storm numbers due to either internal climate dynamics or variations in external forcing. As a result, our uncertainty estimates are likely to be underestimated. However, correcting the uncertainty estimates for long time-scale variability is not straightforward, and would require detailed basin-specific studies that consider the relevant processes driving long-term variability in each region. We now discuss the two methods we use for estimating the mean frequency distribution in more detail.

2.4. Bayesian Analysis with Poisson Assumption

The Poisson distribution is often used to model annual TC numbers (see, for example, Tippett et al. (2011)) and has the benefit of being convenient to use. Based on a Poisson assumption, we apply standard Bayesian methods to derive a posterior distribution for the Poisson parameter. This posterior distribution is an estimate of the mean frequency distribution that we require. The Poisson distribution is one of the few distributions for which there is an uncontroversial and unique objective Bayesian method for deriving posterior distributions. The method uses an objective prior which is proportional to one divided by the square root of the unknown frequency, and results in a posterior for the mean frequency that is gamma distributed. Bernardo and Smith (1993), page 437, gives expressions for the prior and exact closed-form expressions for the posterior for the parameter. The latter corresponds to the mean frequency distribution. The resulting mean frequency distributions are illustrated in Figure 1, for our 12 cases of cat05 and cat45 storms, for six basins.

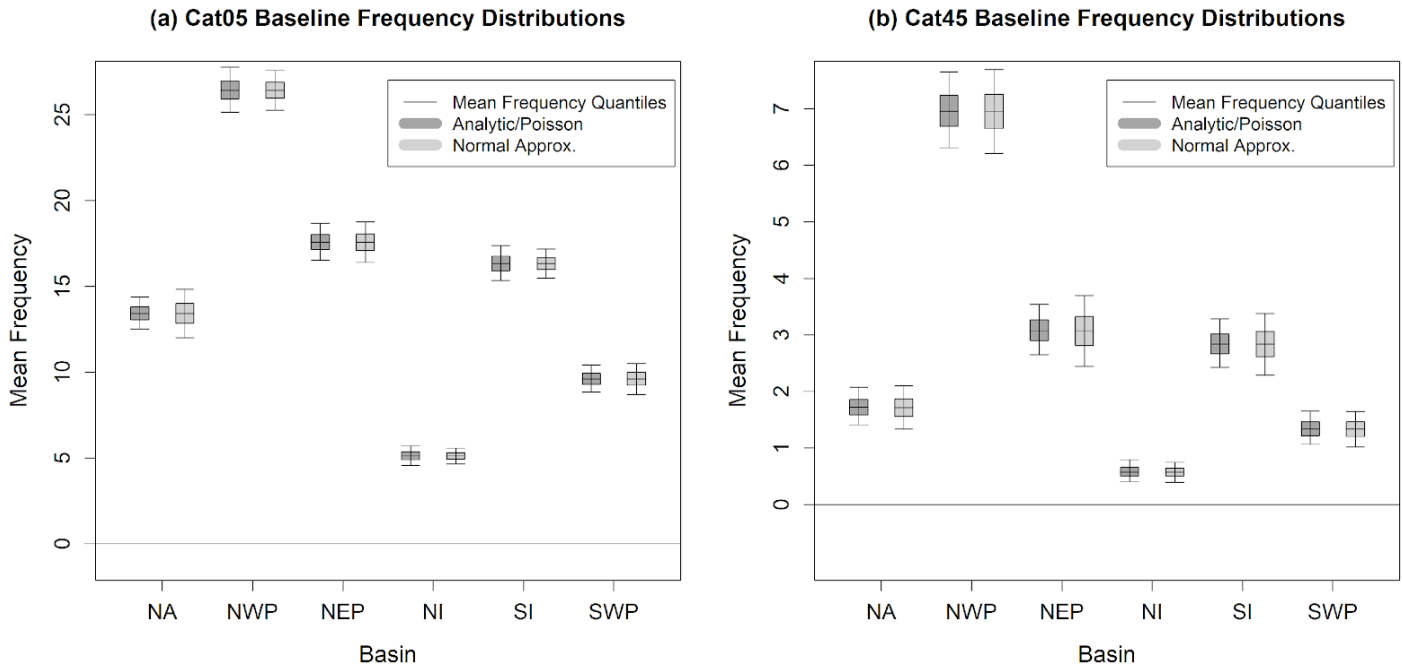


Figure 1: Two estimates for the distributions of uncertainty around the mean frequency of TCs, for each of cat05 (panel (a)) and cat45 (panel (b)), and for each of the six TC basins: North Atlantic (NA), North West Pacific (NWP), North East Pacific (NEP), North Indian (NI), South Indian (SI), South West Pacific (SWP). The two estimates are based on a Poisson assumption for the underlying frequencies (darker grey, left of each pair), and a normal approximation to the posterior (lighter grey, right of each pair). The box-and-whiskers, from bottom to top, show 5%, 25%, 50%, 75% and 95% quantiles of the mean frequency distribution. All estimates are calculated from IBTrACS data, 1980-2021

2.5. Limitations of the Poisson Approach

The exact closed-form expression available for the mean frequency distribution from the Poisson analysis is very convenient. However, the Poisson is not entirely accurate as a model for annual storm numbers, and this may lead to errors in the mean frequency distribution. We evaluate whether the Poisson assumption is appropriate as follows. For the Poisson distribution, the population variance is always equal to the population mean, by definition. In Table 1, column 8, we tabulate the observed ratio of the variance to the mean, a ratio known as the dispersion. For Poisson data we would expect the dispersion to be close to one, and values greater than

one are referred to as overdispersed. We see that for eight out of 12 of our cases the observed dispersions exceed one, seven of them exceed 1.2, and three of them exceed 1.5. This indicates that the Poisson is not a good fit in several of these cases. It may be possible to find distributions that fit the observed TC frequencies better than the Poisson. Good candidates are the negative binomial and ComPoisson distributions, although in our experience even these more flexible distributions are not entirely realistic models for TC frequency. Another possibility would be to model the frequencies as Poisson, but with the Poisson parameter a function of appropriate sea-surface temperature indices using Poisson

regression. For all of negative binomial, ComPoisson and Poisson regression cases, applying the same kind of Bayesian analysis as we have used for the Poisson would be possible, but complex. One of the difficulties is that there would no longer be a unique objective prior, in the way that there is for the Poisson. Another difficulty is that numerical methods would be required to compute the posteriors. The statistical complexity this would introduce to our analysis does not seem justified given that the resulting posterior distributions would still not be entirely realistic, and given the many uncertainties in the overall analysis.

2.6. Normal Approximation to the Posterior Distribution

The second method we use for estimating the mean frequency distribution is to assume that the posterior is normally distributed with a standard deviation given by the estimated standard error of the mean frequency. The use of a normal distribution is reasonably well justified since theoretical results show that parameter posteriors converge to normal distributions as the sample size increases (see Bernardo and Smith (1993), page 291). Given our sample size of 42 years, we can hope that we have achieved relatively good convergence. We estimate the standard error from the data using the standard formula, in which the standard error is the estimated standard deviation divided by the square root of the sample size:

$$\text{Estimated standard error} = \frac{s}{\sqrt{n}}$$

Estimated standard errors for our 12 cases are shown in Table 1, columns 6 and 7. We consider the normal approximation method to be an improvement on the Poisson method, since the standard error is derived from the variance of the actual annual counts, and

therefore accounts for the possibility of overdispersion in the data.

2.7. Comparison of Mean Frequency Distributions

The mean frequency distributions calculated using the normal approximation are shown in Figure 1, and can be compared with the gamma distributed mean frequency distributions from the Poisson analysis. They are relatively similar. For the eight out of 12 cases in which the observed TC counts are overdispersed (see Table 1), the normal approximation mean frequency distributions are wider than the gamma distributed mean frequency distributions. Since the gamma mean frequency distributions seem to be underestimating the uncertainty, we will use the normal approximation mean frequency distributions in our subsequent analysis.

Figure 2a shows the ratio of the standard error to the mean frequency, plotted versus the mean frequency. We will refer to this ratio as the Coefficient of Variation of the baseline uncertainty (CoV-Baseline). CoV-Baseline gives a dimensionless indication of how uncertain the estimated mean frequency is, and we will see later that it relates to whether baseline or climate change uncertainty dominate our projections.

Figure 2a shows that there is a clear relationship such that higher mean frequency typically leads to lower values of the CoV-Baseline. In other words, when there is more data, the mean is estimated more accurately, as would be expected. For this reason, cat05 mean frequencies are generally better estimated than cat45 mean frequencies. This relationship between mean frequencies and CoV-Baseline arises from the properties of the Poisson distribution and the standard error.

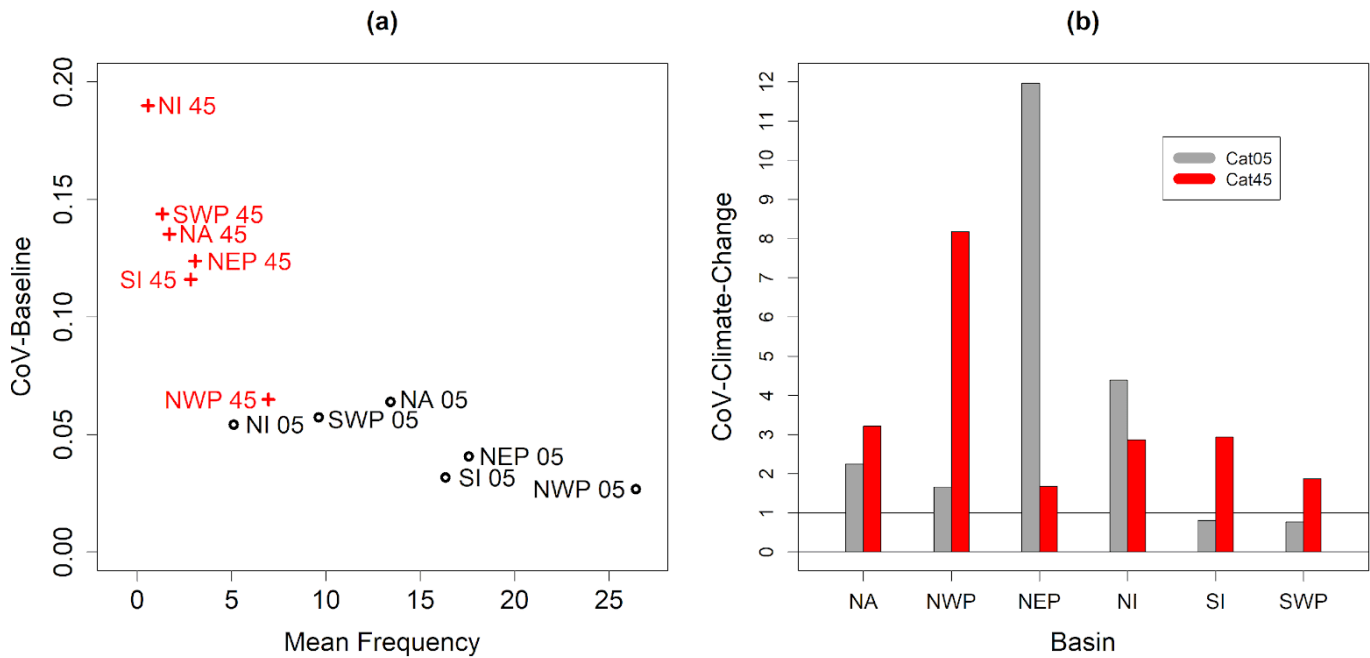


Figure 2: panel (a), horizontal axis: the mean frequency of TCs, estimated from IBTrACS data for the six main TC basins, for Saffir-Simpson Hurricane Wind Scale categories 0-5 (black) and 4-5 (red). Panel (a), vertical axis: the ratio of an estimate of the standard error around the mean frequency to the mean frequency (the CoV-Baseline). Panel (b): all values are derived from the Knutson et al. (2020) projections of TC frequencies, using the post-processing described in the text. Bars show the ratio of the standard deviation of the TC projections to the mean deviation of the TC projections from 1 (the CoV-Climate-Change), for each of the six TC basins. Ratios for category 0-5 storms are shown on the left of each pair, in grey, and ratios for category 4-5 storms are shown on the right of each pair, in red.

3. Climate Change Projections

We derive our projections of climate change from K2020. K2020 collected results from a large number of studies by different authors and generated distributions for how the frequency of cat05 and cat45 TCs may change. The K2020 results are uncertain for many reasons, as the authors discuss. For instance, many of the models on which the K2020 results were based would likely not have simulated particularly realistic TC climates, and so one might doubt their ability to simulate changes in

TC climate under climate change in a realistic way. The K2020 summary results were also derived using various subjective decisions, such as the decision to put equal weights on all the different models considered, even though the models would likely have varied in terms of their ability to simulate the climate. However, in spite of these uncertainties, we have used the K2020 projections because we are not aware that any more credible sets of multi-model projections of future TC frequencies exist at this time. The width of the K2020 distributions represent an estimate of the

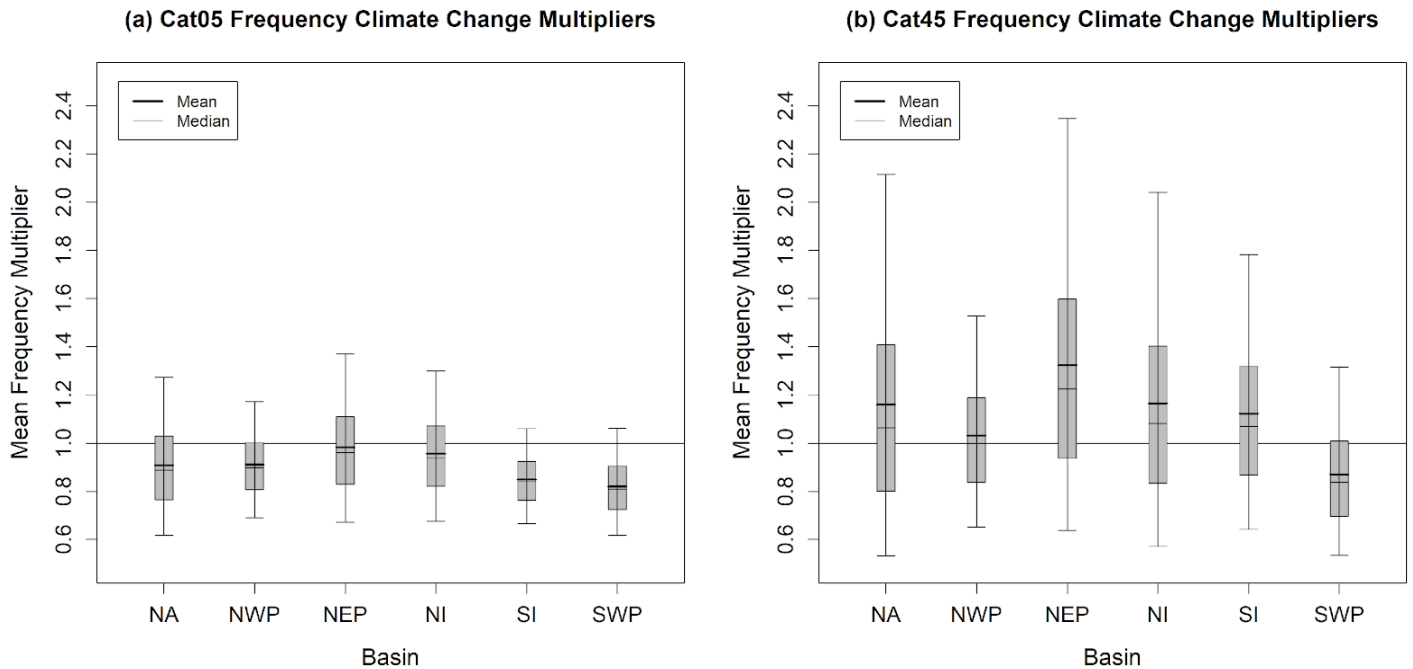


Figure 3: TC frequency projections from Knutson et al. (2020), after applying the post-processing described in the text, for the six major TC basins, as mean frequency multipliers. Panel (a) shows category 0-5 mean frequency changes and panel (b) shows category 4-5 mean frequency changes. The box and whiskers show, from bottom to top, 5% quantile, 25% quantile, median, mean, 75% quantile, 95% quantile.

model uncertainty, based on the set of models they consider. The changes given by K2020 correspond to a 2°C increase in global mean surface temperature (GMST), and are presented using a number of quantiles. We will post-process these distributions to prepare them for our analysis, as follows.

3.1. Post-processing the K2020 Projections

In the first step of post-processing the K2020 projections we fit log-normal distributions to the cat05 and cat45 quantiles to allow us to draw a large number of samples. We fit the distributions using the algorithm described in Jewson (2022). This algorithm ensures that the distributions fitted to the K2020 frequency and mean intensity changes are consistent with respect to the inherent relationships between

cat05 frequency, cat45 frequency and mean intensity.

The distributions of change for cat05 and cat45 frequencies resulting from the distribution fitting process described above are shown in Figure 3. These distributions are similar to the original K2020 results, as shown in figures 1b and 2b in that paper. Small differences between the quantiles of our distributions and the original K2020 quantiles arise from the adjustments we have made in order to reconcile the K2020 frequency and intensity changes in our distribution fitting process.

The distributions of change in Figure 3 are wide, relative to the changes in the mean or median. In several of the 12 cases the differences from a value of one (which represents no change) can be seen to be caused more by the spread of the distribution than by the deviation of the mean or median from one.

The extent to which these distributions of change are dominated by either the change in the mean, or by the spread of the changes, can be quantified by considering the mean-square differences from one (MSD1). The MSD1 can be decomposed into a contribution from the mean squared and a contribution from the variance, as follows:

$$MSD1 = E(d^2) = [E(d)]^2 + V(d) \quad (2)$$

where d is the deviation from one. To illustrate this decomposition, ratios of the standard deviation of change, $\sqrt{V(d)}$, to the mean change, $E(d)$, are given in Figure 2b. We will call this ratio the Coefficient of Variation of the climate change signal (CoV-Climate-Change). CoV-Climate-Change is a non-dimensional measure of the uncertainty around the mean of the climate change projection. We will see later that the CoV-Climate-Change also plays a role, along with the CoV-Baseline, in determining whether baseline uncertainty or climate change uncertainty dominates the uncertainty in our projections.

Values of the CoV-Climate-Change which are less than one indicate that the MSD1 is dominated by a shift in the mean, while values greater than one indicate that the MSD1 is dominated by the variance. We see that for cat05 changes in the South Indian and South West Pacific, the MSD1 is dominated by the mean, but for the other 10 cases it is dominated by the variance. In four cases the CoV-Climate-Change is greater than $\sqrt{10}$, which corresponds to less than 10% of the MSD1 coming from the $[E(d)]^2$ term in Equation (2). In these cases, the distribution is dominated by the variance of the change to a large extent.

The final step of post-processing the K2020 results is to interpolate and extrapolate the changes in cat05 and cat45 frequencies in time, using the method described in Jewson (2021a). This method models the logarithm of the TC frequency as a linear function of global mean surface temperature, following K2020.

This temporal interpolation gives projections of changes in frequency for any RCP and any point in time, relative to the mean frequency during our chosen baseline from 1980 to 2021. The temporal interpolation assumes that the frequency of storms gradually changes from year to year due to climate change during the baseline itself. It therefore allows us to estimate the implied effects of climate change on any year, before, during, or after the baseline period.

We choose not to make projections for mean intensity in this study, since Jewson (2022) has shown that the K2020 changes in mean intensity can be derived from the changes in frequency. Mean intensity projections, if required, could be derived from the mean frequency results we will present.

4. Climate Projections

We now combine the mean frequency distributions described in Section 2 with the distributions for the possible changes due to climate change described in Section 3 to create estimates of actual future TC frequencies. We create $N = 100,000$ samples independently from both distributions and combine them using the expression

$$y(t) = k(t) x \quad (3)$$

where x are samples from the normally distributed mean frequency distribution with standard deviation given by the standard error s/\sqrt{n} ; $k(t)$ are samples from the interpolated climate change uncertainty distribution, which are a function of time t ; and $y(t)$ are the resulting samples from the projected future climate, also as a function of time. The distribution of $y(t)$ is a new mean frequency distribution, now for future climate. Using 100,000 samples gives good convergence of the distribution for $y(t)$.

Figure 4 shows the resulting distributions of the values of the future climate mean frequency distribution, for a 2°C change in GMST, along with the corresponding baseline mean frequency distribution from Figure 1.

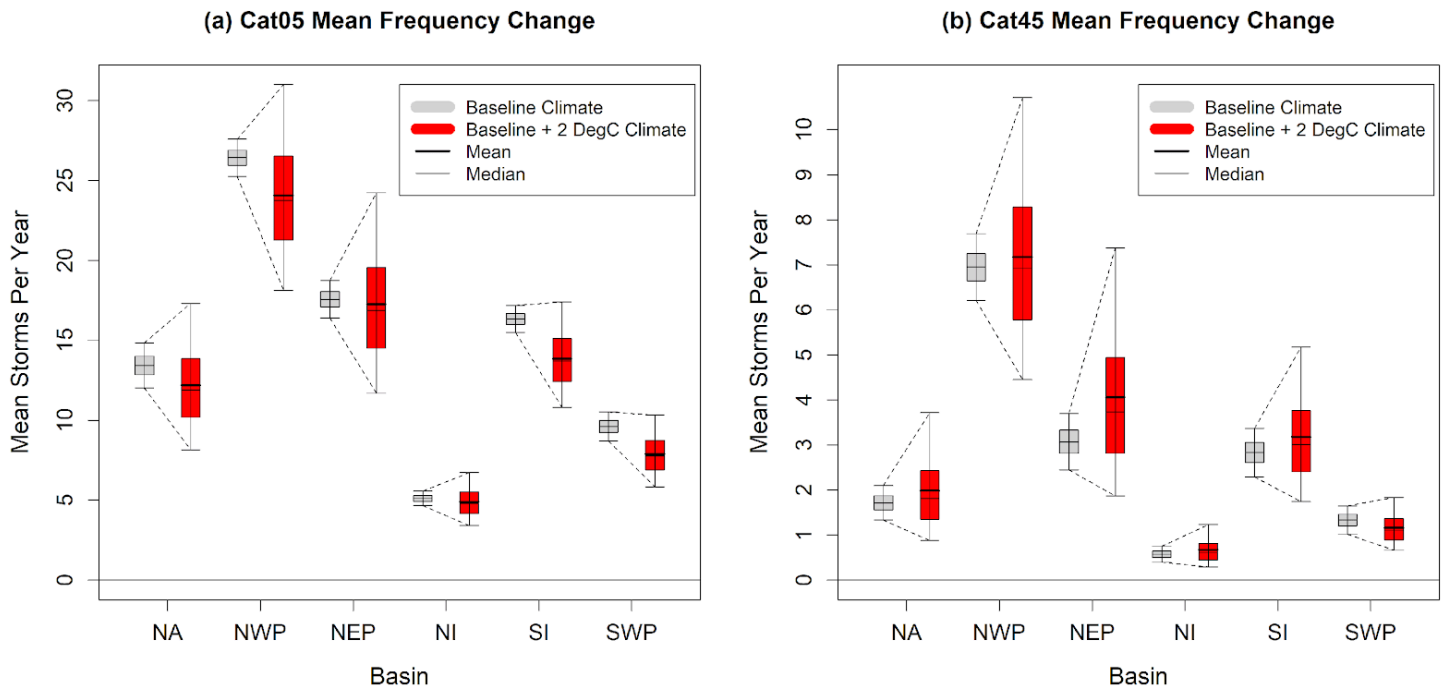


Figure 4: Probabilistic projections of mean frequency of TCs, for the six main TC basins, for category 0-5 and category 4-5 storms. The baseline climate is derived from IBTrACS and follows the normal approximation results shown in Figure 1 (grey). The projections are for a future climate that is warmer by 2°C of global mean surface temperature (red). Box and whiskers for the baseline climate show 5%, 25%, 50%, 75% and 95% quantiles of the baseline mean frequency distribution. Box and whiskers for the projected climate show the same quantiles, and also the mean, of the projected mean frequency distribution. For the baseline climate the mean and median are equal as we are using a normal distribution.

The changes in the median of the twelve distributions are as might be expected from the median frequency changes given in Figure 3. This is not surprising, although mathematically it is not the case that the median of the product of two random variables is necessarily the product of the two medians, and hence the change in the median frequency is not necessarily the same as the change in frequency implied by the median percentage change. For all six basins, the cat05 median frequencies reduce. For all basins except the two West Pacific basins, the cat45 medians increase, while for the two West Pacific basins, the cat45 medians reduce. The projected means are all higher

than the medians, because the distributions of change, and hence the projections, are positively skewed. In some cases the difference between median and mean change is large, e.g., in the North Atlantic for cat45 the mean change is roughly twice the size of the median change. For some risk metrics, it is the mean change which is the more important of the two: Jewson (2021b) shows that it is the mean change which determines the tail behaviour of the distribution of annual maximum wind-speed.

Figure 4 shows the changes in the 5% and 95% quantiles of the mean frequency distribution using diagonal dotted lines. The 75% and 95% quantiles of

the cat05 mean frequency distributions change in different ways from the median in several cases. Two of the 75% quantiles show increases, and five of the 95% quantiles show increases, even though the medians show decreases. In other words, in these cases, the extreme quantiles change in the opposite direction to the median. This is because the distribution becomes so much wider, due to the large uncertainty in the climate change projections.

These results show that considering only the median or mean changes does not give an accurate picture of the possible changes in the distribution. This is because several of the distributions of change are dominated by uncertainty, as illustrated by the large values of the CoV-Climate-Change, as discussed above. It has been reported that TC frequencies are projected to decrease (IPCC, 2022). Our cat05 results agree with that statement on average over the distribution of possible changes, but also project that the extreme quantiles of the distribution of changes increases. In other words, the worst case scenarios for the future climate are worse than at present. This counterintuitive result, which is a consequence of uncertainty, suggests that describing projected changes in TC frequencies as decreases is perhaps an over-simplification.

5. Variance Decomposition

We can seek to better understand the future climate projections shown in Figure 4 by considering the expectation and variance of Equation (3). Taking the expectation of Equation (3), and using the standard expression for the expectation of a product of independent random variables, gives

$$E(y(t)) = E(k(t)x) = E(k(t))E(x) = E_k E_x \quad (4)$$

where we have written $E_k = E(k(t))$, the mean of the frequency change, and $E_x = E(x)$, the mean of the baseline frequency.

We see that the mean of the projection of future climate is equal to the mean of the baseline distribution, multiplied by the mean of the climate change distribution. As mentioned above, there is no analogous relationship for the median, which can make median changes difficult to interpret. Taking variances of Equation (3) and using the standard expression for the variance of a product of independent random variables gives

$$\begin{aligned} V(y(t)) &= V(k(t)x) = [E(k(t))]^2 V(x) + V(k(t))[E(x)]^2 + V(k(t))V(x) \\ &= E_k^2 V_x + V_k E_x^2 + V_k V_x \end{aligned} \quad (5)$$

where we have written $V_k = V(k(t))$, the variance of the frequency change, and $V_x = V(x)$, the variance of the mean baseline frequency (i.e., the standard error squared). We see that the variance of the projection decomposes into three terms. The first term ($E_k^2 V_x$) can be described as the impact of the baseline uncertainty; the second term ($V_k E_x^2$) can be described as the impact of the climate change uncertainty, and the third term ($V_k V_x$) is an interaction term involving both baseline uncertainty and climate change uncertainty.

Figure 5 shows how the three terms on the right hand side of Equation (4) sum to create the total variance – for the cat05 changes – for RCP6.0 (Meinshausen, et al., 2011). The changes at different times are created by temporal interpolation of the results in Figure 4, under the RCP6.0 scenario, using the method from Jewson 2021a. Figure 6 shows the same as Figure 5, but for cat45.

We see that the contribution from the interaction term is small in all cases and can be ignored. For all 12 cases, the baseline uncertainty is initially higher than the climate change uncertainty, but at some point the climate change uncertainty overtakes the baseline uncertainty.

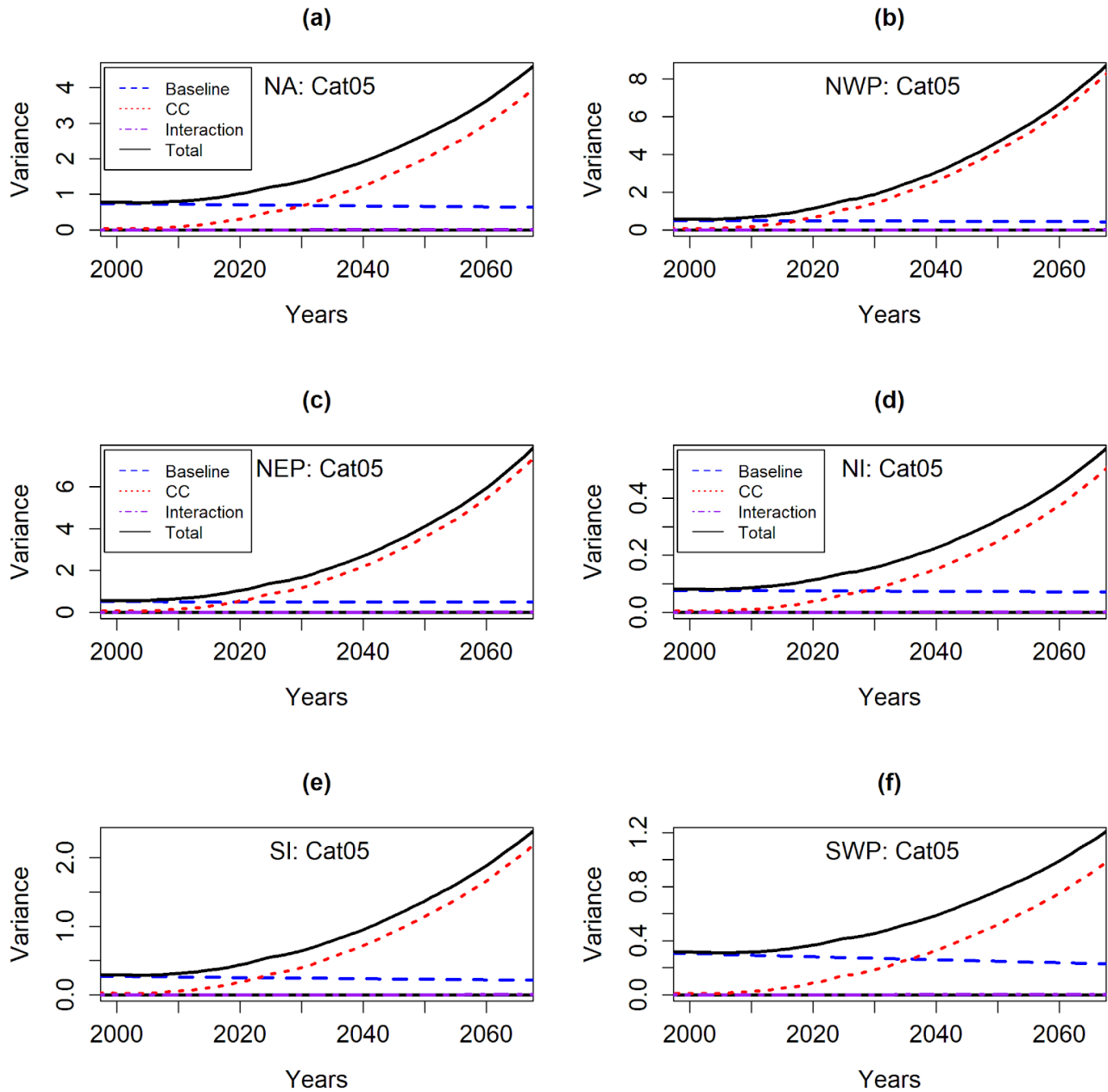


Figure 5: Variances of the uncertainty around projections of future climate for the six main TC basins, for category 0-5 TC frequencies. Total variance (black solid) is the sum of the other three lines, which are the variance related to baseline uncertainty (blue dashed), the variance related to climate change (red dotted) and the variance related to the interaction of the other two variances (purple dot-dashed). The interaction line shows very small values, and is mostly coincident with the zero line.

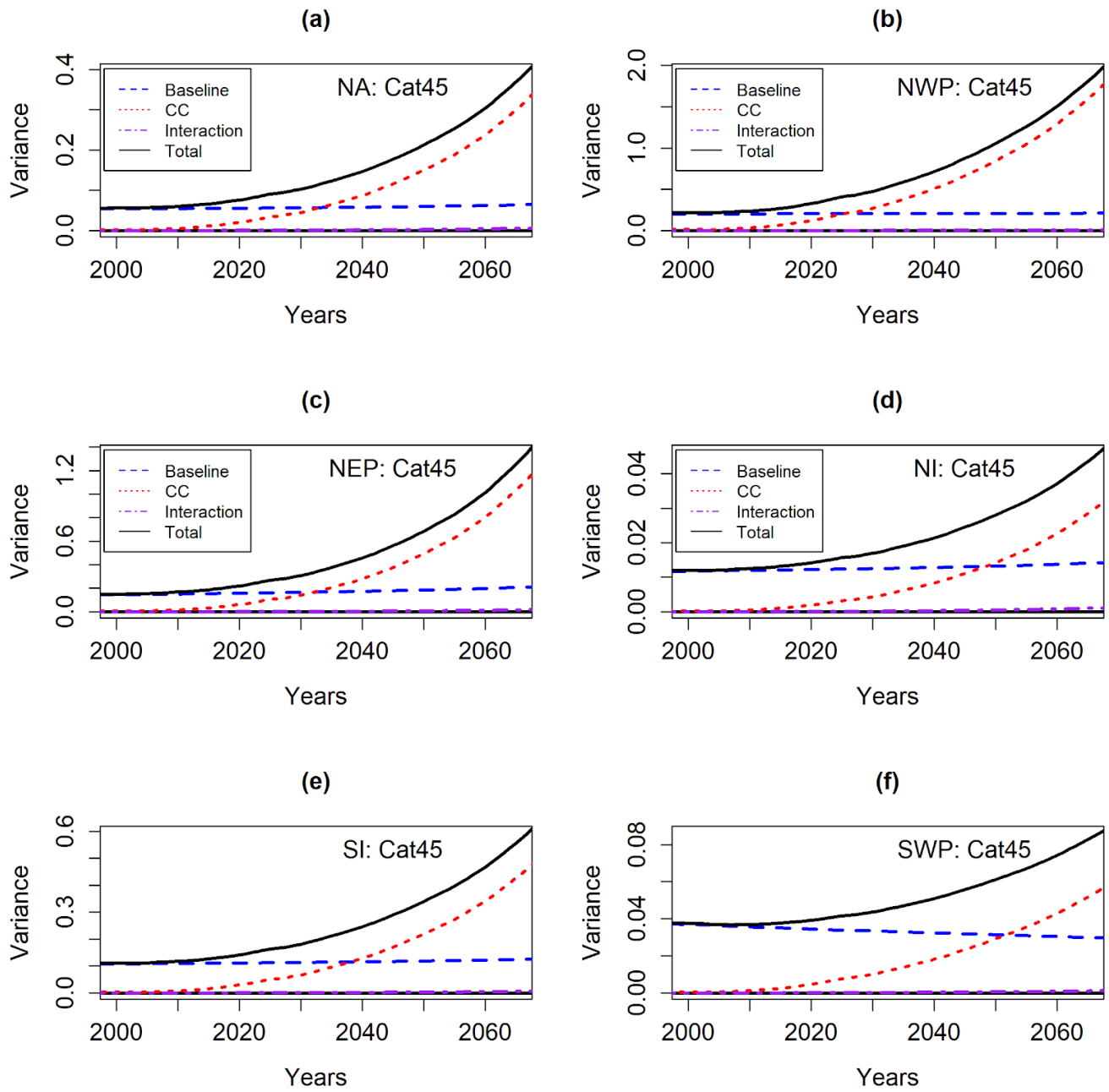


Figure 6: As Figure 5, but now for category 4-5 storms.

We first consider near-term (i.e., 2025) TC conditions. For certain applications of climate information, such as insurance risk quantification, estimates of near-term climate are the most useful. Considering first cat05 projections, we see that baseline and climate change uncertainty are relatively similar, with baseline uncertainty dominant in the North Atlantic, North Indian, and South West Pacific basins, but with climate change uncertainty dominant in the North West Pacific, North East Pacific, and South Indian basins. Considering cat45 projections, we see that baseline uncertainty dominates in all cases except the North West Pacific, where baseline and climate change uncertainty are equal.

We can also assess the point in time at which climate change uncertainty overtakes baseline uncertainty. This point varies from basin to basin and with intensity. Considering cat 05 storms: climate change uncertainty overtakes baseline uncertainty in around 2015 in the North West Pacific, around 2020 in the North East Pacific, and around 2023 in the South Indian. These are therefore cases where climate change uncertainty has already become the larger of the two uncertainties. Climate change uncertainty overtakes baseline uncertainty around the year 2030 in the North Indian and North Atlantic, and late in the 2030s in the South West Pacific. Considering cat45 storms: climate change uncertainty overtakes baseline uncertainty in the 2020s in the North West Pacific, the 2030s in the North Atlantic, North East Pacific and South Indian, in the 2040s in the North Indian, and in the 2050s in the South West Pacific.

The differences between the results from different basins, and between cat05 and cat45 storms, are related to the coefficients of variation given in Figure 3, as follows. We define the ‘climate change uncertainty ratio’ as the ratio of the second to the first terms in Equation 4, evaluated for a 2°C increase in GMST.

This ratio is a measure of the climate change uncertainty, relative to the baseline uncertainty, and is given by

$$\begin{aligned} \text{climate change uncertainty ratio} &= \frac{\text{climate change uncertainty}}{\text{baseline uncertainty}} \\ &= \frac{V_k E_x^2}{E_k^2 V_x} = \frac{V_k}{E_k^2} \frac{E_x^2}{V_x} = \frac{(\text{CoV-climate-change})^2}{(\text{CoV-baseline})^2} \end{aligned} \quad (6)$$

From Figure 2 we see that the North East Pacific cat05 storms have a low CoV-Baseline and the highest CoV-Climate-Change. This gives a high value for the climate change uncertainty ratio. Given the smooth variation of the climate change and baseline variances in time, which is a result of the temporal interpolation, the value of this ratio at 2°C influences the values at all other times. The high value of the ratio is therefore related to why the climate change uncertainty dominates so early on for the North East Pacific cat05 storms, as seen in Figure 5. The low CoV-Baseline for the North East Pacific for cat05 storms is related to the high mean frequency (see Figure 2a). This shows that situations in which the mean frequency is high are likely to show a higher value of the climate change uncertainty ratio and a greater relative impact of climate change uncertainty, because the baseline uncertainty tends to be low. At the opposite end of the range, the South West Pacific cat05 storms have the lowest CoV-Climate-Change. This gives a low value for the climate change uncertainty ratio, and relates to why baseline uncertainty dominates for so long for cat05 storms in the South West Pacific.

Figure 7 quantifies in more detail the extent to which climate change impacts estimates of near-term (2025) climate in our projections. Since we are using a baseline from 1980 to 2021, midpoint 2000/2001, the changes in Figure 7 can be interpreted, roughly speaking, as a change over a 25-year period. The mean changes are relatively small, all less than 5%.

They are all smaller than the corresponding baseline standard errors given in Table 1. The changes in uncertainty (here measured using the change in the standard deviation of the mean frequency distribution for 2025) are larger, and in 10 of the 12 cases exceed 10%.

For the North East and North West Pacific the uncertainty changes are particularly large. For these two basins the main impact of climate change is the increase in uncertainty, rather than the change in the mean.

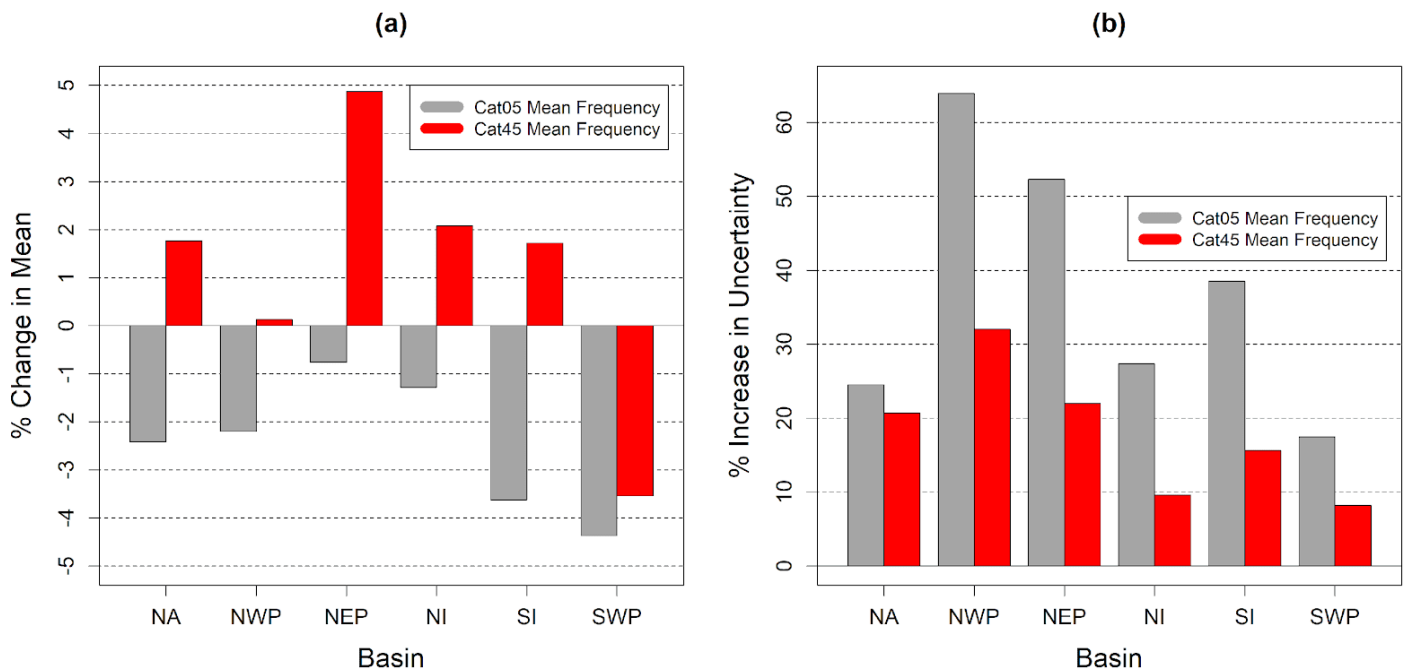


Figure 7: Panel (a): projected change in the mean frequency of TCs for the six main TC basins, for the year 2025, relative to the baseline 1980-2021, based on Knutson et al. (2020) projections, post-processed as described in the text. Panel (b): increase in the standard deviation of the uncertainty (i.e., standard error) around estimates of the mean frequency of TCs over the same time period. In both panels, category 0-5 storms are shown on the left of each pair in grey and category 4-5 storms are shown on the right of each pair in red.

6. Discussion and Uncertainties

These results give useful insights into two of the main drivers of uncertainty around estimates of present and future TC frequency: baseline uncertainty, and climate change uncertainty. However, there are many caveats and uncertainties related to this work and the results. Some of the most critical uncertainties are as follows:

- (a) we have only considered the US representative agency data from IBTrACS. In some basins the data from other agencies is materially different, and if we were to repeat our analysis with these different data sets we would get somewhat different results;
- (b) we have assumed that measuring techniques and reporting practices have remained constant during the period of data that we have used, which is unlikely to be completely correct;
- (c) the intensities of storms in the IBTrACS data that we have used may not be correct, which would then affect our baseline uncertainty estimates;
- (d) our estimation of baseline uncertainty does not account for possible auto-correlation of TC numbers from year to year, and hence we may underestimate baseline uncertainty in some basins;
- (e) historical TC behaviour during parts of the baseline period may have been affected by aerosol concentrations which have subsequently changed (Dunstone et al. (2013), Sobel et al. (2019), Murakami (2022)) leading to a bias which is not accounted for either in the estimates of the baseline or in the K2020 results;
- (f) the K2020 results are based on climate models that may not simulate realistic changes under climate change; and
- (g) to interpolate the K2020 results in time, we have assumed, following K2020, that TC frequencies change as a function of GMST, which may be a poor approximation.

These uncertainties are large enough that future analyses may give qualitatively and quantitatively different results.

For instance, the relativities among the CoVs for both the baseline and climate change inputs could be very different. That would then lead to different conclusions about whether baseline uncertainty or climate change uncertainty dominates at different points in time. The conclusion that both uncertainties are important, is, however, unlikely to change.

We have considered future risks, evaluated today. Future risks, evaluated in the future, will look different. As time progresses, we would expect that baseline uncertainty will reduce, as more historical data accumulates. Also, the baseline will gradually start to incorporate more of the changes due to climate change. Finally, climate change uncertainty estimates may reduce as climate models improve.

We have only considered basin frequencies, although it is landfalling storms which have the most societal impact. The relationship between changes in basin frequencies and changes in landfall frequencies is not simple. Firstly, the possibility that storms with cat45 intensity may make landfall with a lower intensity than cat45 complicates the application of basin frequency changes to landfalling storms. Second, climate change may change where storms form, and the tracks they take, and those effects may be a more important factor in determining how landfall frequencies change than changes in basin frequency (Knutson, et al., 2022). Given these two considerations, our results should not be applied to landfall frequencies. Performing a similar analysis of the drivers of uncertainty for frequencies of landfalling storms is an important subject for future work. Landfalling storms have lower mean frequencies than basin storms, and we have seen that lower mean frequencies lead to higher values of the CoV-Baseline, and hence a more important role for baseline uncertainty. We might therefore anticipate that baseline uncertainty will play a more important role for landfalling storm frequencies than it does for basin storm frequencies.

7. Summary and Conclusions

We have made probabilistic projections of future tropical cyclone (TC) frequencies by combining probabilistic estimates of a baseline TC climate with probabilistic estimates of how TC climate may change. The baseline climate estimates are based on statistical analysis of historical TC observations for the period 1980-2021. The climate change estimates are derived, via some steps of post-processing (as described above), from the meta-study of climate model outputs presented by Knutson et al. (2020). We make projections for Saffir-Simpson Hurricane Wind Scale category 0-5 (cat05) and category 4-5 (cat45) frequencies for all six major TC basins.

For cat05 frequencies, considering changes corresponding to a 2°C increase in global mean surface temperature (GMST), we find that the median projected frequencies are all lower than the median baseline frequencies. However, for two basins, the 75% quantile of the projected frequencies is higher than the 75% quantile for the baseline, and for five basins, the 95% projected quantile is higher than the 95% quantile for the baseline. This is driven by the large uncertainty in the climate change results, and indicates that the projected changes in cat05 frequencies should be considered as being more complex than just a decrease in frequency.

For cat45 frequencies, also for a 2°C increase in GMST, we find that the median projected frequencies are higher than the median baseline frequencies, for five out of six basins. For the South West Pacific they are lower. For the North East Pacific, the projected frequencies are dramatically higher, and the projected median is higher than the 95% quantile for the baseline.

We use the product of variances formula to decompose the uncertainty of the projections into three components: baseline uncertainty, projection uncertainty and an interaction term. The interaction term turns out to be negligible. For climate in the year 2000, baseline uncertainty is larger than climate

change uncertainty in all cases. However, for three basins we find that for the frequency of cat05s, climate change uncertainty has already (in 2024) overtaken baseline uncertainty. For the other cases, under RCP6.0, climate uncertainty overtakes baseline uncertainty at different points between 2020 and 2060. For climate in the year 2025, the mean frequencies of storms change by less than 5% in all cases, relative to the baseline. However, the standard deviation around the mean (the standard error) of storm frequencies increases by much larger amounts in several cases. For these cases, the change in the uncertainty is the dominant impact of the climate change projections.

The climate change uncertainty is large: this is driven by disagreement among climate models. As climate models improve, this uncertainty will hopefully reduce. The baseline uncertainty is also large: this is driven by the limited number of years of satellite data that we have to estimate the baseline. Assuming satellite observations are maintained, this will gradually reduce, although the root-n rule suggests it will take more than 150 years for it to reduce to half of the current level.

We have discussed many sources of uncertainty in these results. Some of these uncertainties could be reduced by performing basin specific studies. However, many of the uncertainties are irreducible, and decision makers must embrace these uncertainties in their decision making process.

Effective adaptation to climate change requires quantitative estimates of future risks. Such estimates should include quantification of as many of the material sources of uncertainty as possible. Much of the literature on future TC frequencies ignores the role of baseline estimation uncertainty. The methodology we have used here demonstrates how baseline estimation uncertainty can be incorporated into estimates of future TC frequencies, and the results show that it is material. We would therefore encourage risk modellers to model baseline estimation uncertainty in their risk models.

References

- Arthur, W., 2021. A statistical–parametric model of tropical cyclones for hazard assessment. *NHESS*, Volume 21, p. 893–916.
- Bernardo, J. & Smith, A., 1993. *Bayesian Theory*. New York: Wiley.
- Bhatia, K. et al., 2019. Recent increases in tropical cyclone intensification rates. *Nature Communications*, Volume 10.
- Bloemendaal, N. et al., 2022. A globally consistent local-scale assessment of future tropical cyclone risk. *Science Advances*, Volume 8.
- Bloemendaal, N. et al., 2020. Generation of a global synthetic tropical cyclone hazard dataset using STORM. *Scientific Data*, Volume 7.
- Clark, K., 1986. A formal approach to catastrophe risk assessment and management. *Proceedings of the Casualty Actuarial Society*, Volume 73, pp. 69-92.
- Coughlin, K. et al., 2009. A relationship between all Atlantic hurricanes and those that make landfall in the USA. *Quarterly Journal of the Royal Meteorological Society*, Volume 135, pp. 371-379.
- Dunstone, N. J. et al., 2013. Anthropogenic aerosol forcing of Atlantic tropical storms. *Nature Geoscience*, Volume 6, pp. 534-539.
- Elsner, J. & Jagger, T., 2006. Prediction models for annual U.S. hurricane counts. *Journal of Climate*, 19(12), p. 2935–2952.
- Emanuel, K., 2020. Response of Global Tropical Cyclone Activity to Increasing CO₂: Results from Downscaling CMIP6 Models. *Journal of Climate*, Volume 34, pp. 57-70.
- Emanuel, K., Ravela, S., Vivant, E. & Risi, C., 2006. A statistical deterministic approach to hurricane risk assessment. *BAMS*, Volume 87, pp. 299-314.
- Friedman, D., 1972. Insurance and the Natural Hazards. *ASTIN*, Volume 7, pp. 4-58.
- Friedman, D., 1975. *Computer Simulation in Natural Hazard Assessment*. Colorado: University of Colorado.
- FSBoA, 2022. *Florida Commission on Hurricane Loss Projection Methodology*. [Online] Available at: <https://www.sbafla.com/method/Home.aspx> [Accessed 4 4 2022].
- Garner, A., Kopp, R. & Horton, B., 2021. Evolving Tropical Cyclone Tracks in the North Atlantic in a Warming Climate. *Earth's Future*, Volume 9.
- Grieser, J. & Jewson, S., 2012. The RMS TC-rain model. *Meteorologische Zeitschrift*, Volume 21, pp. 79-88.

- Hall, T. & Jewson, S., 2007. Statistical modeling of North Atlantic Tropical Cyclone Tracks. *Tellus*, Volume 59A, pp. 486-498.
- Hassanzadeh, P. et al., 2020. Effects of climate change on the movement of future landfalling Texas tropical cyclones. *Nature Communications*, Volume 11.
- IPCC, 2022. *Climate Change 2021: The Physical Science Basis: Technical Summary*. Cambridge: CUP.
- Jagger, T. & Elsner, J., 2006. Climatology Models for Extreme Hurricane Winds near the United States. *Journal of Climate*, Volume 19, p. 3220–3236.
- Jewson, S., 2023. The Impact of Projected Changes in Hurricane Frequencies on U.S. Hurricane Wind and Surge Damage. *JAMC*, 62(12), p. 1827–1843.
- Jewson, S., 2021a. Conversion of the Knutson et al. Tropical Cyclone Climate Change Projections to Risk Model Baselines. *JAMC*, Volume 60, p. 1517–1530.
- Jewson, S., 2021b. Interpretation of the Knutson et al. (2020) hurricane projections, the impact on annual maximum wind-speed, and the role of uncertainty. *SERRA*, pp. 1-17, <https://doi.org/10.1007/s00477-021-02142-6>.
- Jewson, S., 2022. Application of uncertain hurricane climate change projections to catastrophe risk models. *Stoch Environ Res Risk Assess*, Volume 2022, <https://doi.org/10.1007/s00477-022-02198-y>.
- Jewson, S., 2022. The Interpretation and Implications of the Knutson et al. 2020 Projections of Changes in the Frequency and Intensity of Tropical Cyclones Under Climate Change. *QJRM*S, Volume (in print), pp. tbd, <https://doi.org/10.1002/qj.4299>.
- Jewson, S. et al., 2007. Five Year Prediction of the Number of Hurricanes that make United States Landfall. In: J. Elsner, ed. *Hurricanes and Climate Change*. Boston: Springer.
- Kaczmarska, J., Winter, H., Arfeuille, F. & Bellone, E., 2022. Estimating North Atlantic Hurricane Landfall Counts and Intensities in a Non-stationary Climate. In: *Hurricane Risk Volume 2*. Boston: Springer, pp. 57-86.
- Knapp, K. et al., 2010. The International Best Track Archive for Climate Stewardship (IBTrACS): Unifying tropical cyclone best track data.. *BAMS*, Volume 91, pp. 363-376.
- Knutson, T. et al., 2020. Tropical cyclones and climate change assessment: Part II: projected response to anthropogenic warming. *BAMS*, 101(3), pp. E303-E322.
- Knutson, T. et al., 2019. Tropical cyclones and climate change assessment: Part 1: detection and attribution. *BAMS*, 100(10), pp. 1987-2007.
- Knutson, T. et al., 2022. Dynamical downscaling projections of late twenty-first-century U.S. landfalling hurricane activity. *Climatic Change*, Volume 171.

- Kossin, J., Knapp, K., Olander, T. & Velden, C., 2020. Global Increase in major tropical cyclone exceedance probability over the past four decades. *PNAS*, 117 (22), pp. 11975-11980.
- Lee, C., Tippett, M., Sobel, A. & Camargo, S., 2018. An Environmentally Forced Tropical Cyclone Hazard Model. Volume 10, pp. 223-241.
- Liu, M., Vecchi, G., Smith, J. & Knutson, T., 2019. Causes of large projected increases in hurricane precipitation rates with global warming. *npj Climate and Atmospheric Science*, Volume 2.
- Meiler, S. et al., 2023. Uncertainties and sensitivities in the quantification of future tropical cyclone risk. *Communications Earth & Environment*, 4(1).
- Meinshausen, M. et al., 2011. The RCP greenhouse gas concentrations and their extensions from 1765 to 2300. *Climatic Change*, Volume 109.
- Murakami, H., 2022. Substantial global influence of anthropogenic aerosols on tropical cyclones over the past 40 years. *Sci. Adv.*, Volume 8.
- Murakami, H. et al., 2020. Detected climatic change in global distribution of tropical cyclones. *Proceedings of the National Academy of Sciences. U.S.A.*, Volume 117, pp. 10706-10714.
- Sobel, A., Camargo, S. & Previdi, M., 2019. Aerosol versus Greenhouse Gas Effects on Tropical Cyclone Potential Intensity and the Hydrologic Cycle. *Journal of Climate.*, Volume 32, pp. 5511-5527.
- Sobel, A. et al., 2021. Tropical Cyclone Frequency. *Earth's Future*, Volume 9.
- Stansfield, A., Reed, K. & Zarzycki, C., 2020. Changes in Precipitation From North Atlantic Tropical Cyclones Under RCP Scenarios in the Variable-Resolution Community Atmosphere Model. *GRL*, Volume 47.
- Sun, Y. et al., 2017. Impact of Ocean Warming on Tropical Cyclone Size and Its Destructiveness. *scientific reports*. 7, 8154.
- Ting, M., Kossin, J. & Camargo, S., 2019. Past and future hurricane intensity change along the U.S. East Coast. *Sci Rep*, Volume 9.
- Tippett, M., Camargo, S. & Sobel, A., 2011. A Poisson Regression Index for Tropical Cyclone Genesis and the Role of Large-Scale Vorticity in Genesis. *Journal of Climate*, Volume 24, p. 2335–2357.
- Tolwinski-Ward, S., 2015. Uncertainty quantification for a climatology of the frequency and spatial distribution of North Atlantic tropical cyclone landfalls. *Journal of Advances in Modeling Earth Systems*, Volume 7, p. 305–319.
- Vickery, P., Skerlj, P. & Twisdale, L., 2000. Simulation of Hurricane Risk in the US Using Empirical Track Model. *Journal of Structural Engineering*, Volume 126.

- Villarini, G., Vecchi, G. & Smith, J., 2012. U.S. landfalling and North Atlantic hurricanes: statistical modeling of their frequencies and ratios. *Monthly Weather Review*, 140(1), p. 44–65.
- Walsh, K. et al., 2015. Tropical cyclones and climate change. *Wires Climate Change*, Volume 7, pp. 65-89.
- Yamaguchi, M. et al., 2020. Global warming changes tropical cyclone translation speed. *Nature Communications*, Volume 11.
- Zhang, G., Murakami, H., Knutson, T. & Yoshida, K., 2020. Tropical cyclone motion in a changing climate. *Science Advances*, Volume 6.
-

Data Availability Statement

The data from Knutson *et al.* (2020) is available at <https://doi.org/10.5281/zenodo.4738905>.

The IBTrACS data used in this study is available from <https://www.ncdc.noaa.gov/IBTrACS/>

Declarations

Funding: Lambda Climate Research Ltd is funded by a consortium of insurance companies.

Conflicts of interest: The author is the owner of Lambda Climate Research Ltd, a think tank that researches weather and climate risk.

Handling Editor: Adam Sobel, Professor, Columbia University

The *Journal of Catastrophe Risk and Resilience* would like to thank Adam Sobel for his role as Handling Editor throughout the peer-review process for this article. We would also like to extend our thanks to the chosen academic reviewers for sharing their expertise and time while undertaking the peer review of this article.

Received: February 22, 2024

Accepted: June 12, 2024

Published: July 23 2024

Rights And Permissions

Access: This article is Diamond Open Access
Licensing: [Attribution 4.0 International \(CC BY 4.0\)](https://creativecommons.org/licenses/by/4.0/)

DOI: <https://doi.org/10.63024/m9wk-3420>

Article Number: 1.01

ISSN: 3049-7604

Copyright: Copyright remains with the author, and not with the *Journal of Catastrophe Risk and Resilience*.

Article Citation Details

Jewson, S., 2024. Projecting future tropical cyclone frequencies by combining uncertain empirical estimates of baseline frequencies with climate model estimates of change, *Journal of Catastrophe Risk and Resilience*, Issue 01, Article 01, <https://doi.org/10.63024/m9wk-3420>

Share this article:

<https://journalofcrr.com/research/01-01-Jewson>